Land–water allocation, yield stability and policy trade-offs under climate change: A system dynamics analysis

Xiaojing Jia [1], Ruiqi Zhang [1]

（1 *School of Business, Central University of Finance and Economics, Beijing 100081, China;* ）

Abstract: Global climate change is intensifying hydroclimatic extremes and agricultural water scarcity, sharpening trade-offs among yield stability, water saving and rural incomes in major grain-producing regions. Existing studies often optimise cropping patterns or irrigation schedules in isolation and rarely incorporate yield robustness or explicit policy instruments within a single decision framework. This article develops an integrated machine-learning–system-dynamics–NSGA-II (ML–SD–NSGA-II) framework that links long-horizon meteorological scenarios, crop–water–economy dynamics and multi-objective optimisation of crop areas and irrigation depths.

A set of ML models generates daily climate sequences that drive a system dynamics model of soil moisture, yield formation, basin-scale available water and farm returns; NSGA-II then identifies Pareto-optimal strategies that jointly maximise profit and irrigation water productivity, while minimising yield deviation. Applied to a rice–wheat irrigation system in the middle Yangtze River Basin, the framework identifies “knee-point” strategies that increase irrigation water productivity by approximately 14% relative to the observed baseline while maintaining near-baseline profits and substantially reducing yield deviation.

Scenario analysis under differentiated water pricing, quota-based irrigation subsidies and an extreme-drought analogue shows that, under normal climatic conditions, moderate tariffs mainly curb low-value water use with limited impacts on profit and yield stability. Under extreme drought, however, sharp reductions in effective water availability dominate system behaviour, and prices and subsidies provide only limited buffering effects. The framework therefore offers a transparent quantitative tool for testing coordinated water-pricing and subsidy packages and for informing irrigation-district governance and climate-adaptation policy in monsoon Asia and other water-constrained agricultural regions.

Keywords: climate change; water scarcity; irrigated agriculture; system dynamics; machine learning; multi-objective optimisation

1. Introduction

Agriculture plays a foundational role in global food security and rural livelihoods while remaining the largest consumer of freshwater worldwide, accounting for approximately 70% of global withdrawals and an even higher share in many developing regions (FAO, 2011). Under ongoing climate warming, the frequency and intensity of droughts, floods and compound hot-dry events continue to rise (IPCC, 2021), undermining yield stability and water security in major grain-producing regions (IPCC, 2022). As a result, policymakers are increasingly confronted with a persistent governance dilemma: how to maintain food supply and farm incomes while operating within tightening freshwater constraints and climate uncertainty.

Experiences from major producers and exporters such as Iran, the U.S. Great Plains, India and Brazil suggest that policy strategies centered on irrigated-area expansion and yield maximisation have often intensified pressure on limited blue and green water resource, accelerated groundwater depletion and vulnerability to climatic shocks (Lopes et al., 2021; Madani, 2014; Mall et al., 2006; McGuire, 2014; Steward et al., 2013). These cases highlight that, in an era of more frequent extremes and deep integration with global markets, conventional approaches relying primarily on expanding irrigation to raise technical efficiency struggle to reconcile production stability with finite water availability. The challenge is therefore not only technical but institutional: existing policy instruments may redistribute scarcity without fundamentally resolving the underlying trade-offs.

Within this context, crop planting structure and irrigation water allocation represent two central levers of agricultural water governance. Crops differ substantially in water demand, yield potential and economic returns (Cao et al., 2022), meaning that extensive cultivation of high-water-use, low-value crops aggravate water stress and weakens system resilience (Wu et al., 2025; Xu et al., 2025; Zhang, 2023). Adjusting cropping patterns has been shown to reduce peak irrigation demand and moderate yield volatility under climate shocks (Feng et al., 2024; He et al., 2025). In parallel, irrigation allocation strategies—ranging from critical-growth-stage prioritisation to differentiated water pricing and quota-based subsidies—have been widely promoted to enhance water-use efficiency and steer scarce water towards higher-value uses (Deng and Zhang, 2025; Qi et al., 2025; Reca et al., 2001; Yin et al., 2025).

However, most policy interventions and analytical frameworks continue to address cropping decisions and irrigation management in isolation. Empirical and modelling studies often optimise either crop structure or irrigation scheduling separately, without explicitly representing how land-use decisions, water allocation, soil moisture, yields and farm incomes interact dynamically over time (Feng et al., 2023; Li and Liu, 2020; Su et al., 2024; Zhou et al., 2024). As a result, important feedbacks and trade-offs are obscured, and policies that appear effective under average conditions may perform poorly under climate extremes.

More fundamentally, the effectiveness of commonly used economic instruments—such as volumetric water pricing, tiered tariffs and irrigation subsidies—remains contested under conditions of absolute scarcity. While moderate price increases can suppress low-marginal-benefit water use in normal years, and subsidies can buffer income losses, evidence suggests that these instruments offer only limited protection when water availability collapses during severe droughts (Lesk et al., 2022; Zhao et al., 2024). Under such conditions, efficiency-oriented policies may reallocate scarcity rather than mitigate its impacts, exposing structural limits of existing governance approaches. Yet there remains a lack of quantitative tools that can examine these policy trade-offs dynamically, across interacting land–water systems and under explicit climate uncertainty.

Addressing this gap requires analytical frameworks capable of linking climate variability, land-use decisions, irrigation allocation and economic outcomes within a single dynamic system. System dynamics (SD) has been increasingly used to represent nonlinear feedbacks and delays in agricultural water systems, while machine learning (ML) and multi-objective optimisation have enhanced the ability to explore complex decision spaces and competing objectives (Jamali et al., 2025; Ortuzar et al., 2025; Shi and Guo, 2024). Yet integrated applications that trace how climate uncertainty propagates through soil moisture, yields and farm incomes—and that explicitly treat yield robustness alongside economic returns and water-use efficiency—remain scarce, particularly in monsoon irrigation systems.

This study addresses these challenges by examining land–water allocation and policy trade-offs in a typical rice–wheat irrigation system in monsoon China. Rather than asking how to maximise efficiency alone, we investigate under what conditions coordinated adjustments of cropping structure and irrigation allocation can stabilise yields and incomes, and where economic instruments such as water pricing and subsidies reach their governance limits under extreme climate stress. To do so, we develop an integrated modelling framework that combines climate-scenario generation, dynamic simulation of crop–water–economy interactions and multi-objective decision analysis. The framework is used to compare baseline, policy-adjustment and extreme-drought scenarios, allowing policy instruments to be stress-tested ex ante.

By foregrounding trade-offs between efficiency, stability and income under climate uncertainty, this study contributes to debates in environmental governance on the limits of marginal efficiency improvements and the need for coordinated structural and institutional responses. Empirically, it provides evidence from a major grain-producing region in monsoon Asia, while methodologically offering a transparent tool for evaluating land–water policies in climate-sensitive irrigation systems.

2. Literature review

2.1 Land–water allocation as a governance problem

Land use and irrigation water allocation have long been recognised as central levers in agricultural water governance, particularly in regions facing increasing climate variability and freshwater constraints. A substantial body of research demonstrates that cropping patterns strongly shape water demand, yield outcomes and environmental pressures (Liu et al., 2023; Zou et al., 2025). Adjusting crop-sown areas—by reducing high-water-use crops or introducing seasonally complementary rotations—can smooth irrigation demand, reduce pressure on scarce water resources and mitigate yield volatility (Demir and Muratoglu, 2025; Feng et al.,2024; Li et al., 2024; Shi et al., 2024; Zhou et al., 2024). Diversified cropping systems have also been shown to enhance resilience to droughts and heatwaves by distributing climate risk across crops with different sensitivities (Cao et al., 2025; He et al.,2025).

2.2 Policy instruments and the limits of efficiency-oriented governance

A large share of the literature on agricultural water management assumes that efficiency gains—through improved allocation, pricing or technology—can reconcile competing objectives of production, income and resource conservation. Under average hydrological conditions, moderate water pricing has been shown to suppress low-marginal-benefit irrigation without substantially reducing yields or farm incomes (Deng and Zhang, 2025; Guemouria et al., 2023). Subsidies and quotas are often introduced to offset distributional impacts and maintain political acceptability (Yin et al., 2025).

Yet growing evidence suggests that such instruments face structural limits under conditions of absolute water scarcity and extreme climate events. During severe droughts, when total water availability collapses, price signals alone cannot generate additional supply and may simply redistribute losses among users (Lesk et al., 2022). Similarly, quotas and subsidies may buffer income impacts but cannot fully prevent yield declines when biophysical constraints dominate (Zhao et al., 2024). In these contexts, efficiency-oriented policies risk obscuring deeper governance challenges by focusing on marginal reallocations rather than structural adaptation.

This tension highlights a key gap in the literature: while policy instruments are often evaluated individually, their combined performance under interacting land-use decisions, water constraints and climate extremes remains poorly understood. In particular, there is limited quantitative analysis of how pricing, quotas and subsidies interact with cropping structure to shape yield stability and income outcomes over time.

2.3 Climate uncertainty and dynamic trade-offs in irrigated systems

Climate change adds an additional layer of complexity to land–water governance by increasing uncertainty in both water supply and crop responses. Rising temperatures, altered precipitation regimes and more frequent compound extremes affect crop phenology, evapotranspiration demand and yield variability (Becker et al., 2023; IPCC, 2022). These impacts are not linear: moderate changes may be absorbed through management adjustments, whereas extreme events can trigger abrupt system responses, including sharp yield losses and cascading economic effects (Dong et al., 2022).

Most existing studies examine climate impacts on either yields or water demand in isolation, often using scenario analysis or crop models to estimate average effects (Ghimire et al., 2025; Marcinkowski et al., 2024). While valuable, such approaches tend to overlook feedbacks between land-use decisions, irrigation rules and basin-level water availability. As a result, they provide limited insight into how governance instruments perform under dynamic climate stress, particularly when short-term coping strategies undermine long-term system resilience.

This gap is especially salient in monsoon irrigation systems, where strong seasonality and inter-annual variability amplify the consequences of misaligned land–water decisions. Understanding governance trade-offs in such systems therefore requires analytical frameworks capable of tracing how climate uncertainty propagates through coupled land–water–economy dynamics.

2.4 Modelling approaches for analysing governance trade-offs

System dynamics (SD) has been widely applied to agricultural water systems because of its ability to represent nonlinear feedbacks, delays and accumulation processes. SD models have been used to explore long-term interactions between cropping patterns, irrigation demand, water availability and farm income, and to assess the implications of alternative policy scenarios (Jamali et al., 2025; Jia et al., 2023; Mehrazar et al., 2020; Naeem et al., 2024; Wang et al., 2022). Recent reviews argue that SD-based approaches are particularly well suited for analysing policy trade-offs and unintended consequences in complex socio-environmental systems (Shi and Guo, 2024).

In parallel, machine learning (ML) and multi-objective optimisation have enhanced the capacity to handle high-dimensional decision spaces and competing objectives (Ahmed et al., 2024; Torabi et al., 2024; Ye et al., 2024). Evolutionary algorithms such as NSGA-II are increasingly used to identify Pareto-optimal land–water strategies that balance economic returns, water-use efficiency and environmental outcomes (Ortuzar et al., 2025; Wu et al., 2025). However, many applications remain method-driven, with limited integration of governance questions and insufficient attention to yield robustness under extreme events.

Taken together, the literature points to the need for integrative frameworks that move beyond ex post evaluation of policy scenarios towards ex ante stress-testing of governance instruments. Such frameworks should explicitly link climate uncertainty, land-use decisions, irrigation allocation and economic incentives, and treat yield stability as a core governance concern rather than a secondary outcome.

2.5 Research gap and contribution

Despite extensive research on crop structure optimisation, irrigation allocation and climate impacts, three gaps remain. First, land-use and irrigation decisions are still predominantly analysed in isolation, limiting understanding of their joint governance implications. Second, policy instruments are often evaluated under average conditions, with insufficient attention to their performance limits under extreme climate stress. Third, yield robustness—a central concern for food security and political stability—is rarely treated as an explicit objective in land–water governance analysis.

By addressing these gaps, this study contributes to debates on adaptive water governance under climate change. It provides a quantitative framework for analysing land–water trade-offs and policy limits in a climate-sensitive irrigation system, and offers empirical insights into when efficiency-oriented instruments can stabilise outcomes and when structural constraints dominate.

3. System dynamics modelling

3.1 Conceptual framework and study area

To analyse how land-use decisions, irrigation allocation and economic incentives interact under climate uncertainty, we develop a SD model representing a typical irrigated rice–wheat double-cropping system in a monsoon basin in the middle reaches of the Yangtze River. The region is characterised by strong seasonal concentration of precipitation and high dependence of winter–spring crops on irrigation, features that are representative of rice–wheat systems across monsoon Asia. The case therefore provides a suitable setting for examining governance challenges associated with seasonal water scarcity under climate change.

The model operates at a ten-day (dekad) time step, which corresponds to the practical decision cycle of irrigation scheduling while allowing key crop growth stages and soil-moisture dynamics to be resolved explicitly. Water-related variables are consistently represented in both depth (mm) and volume (million m³), with conversion based on crop-specific sown area. This ensures internal accounting consistency between land-use decisions and basin-scale water

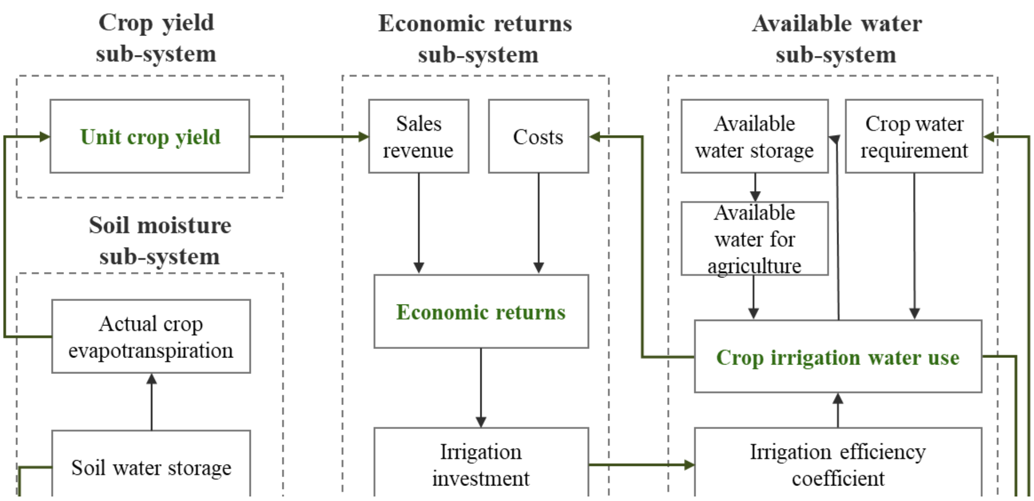

Figure 1 The four sub-systems included in the model

availability.

As illustrated in *Figure 1*, the SD model integrates four tightly coupled sub-systems:

(i) a soil-moisture sub-system that represents root-zone water storage for rice and wheat as stock variables;

(ii) a crop-yield sub-system that translates accumulated water stress over successive growth stages into seasonal yield outcomes;

(iii) an available-water sub-system that represents basin-scale allocable water as a stock and imposes binding supply constraints on irrigation decisions; and

(iv) an economic-return sub-system that accumulates revenue, costs policy transfers over time.

Meteorological variables, including precipitation, temperature, humidity, radiation and wind speed, enter the model as exogenous drivers. Crop-specific sown areas and dekad-level net irrigation depths are treated as decision variables whose trajectories are determined externally by the optimisation module and then introduced into the SD framework. Once introduced, these decision variables endogenously shape soil-moisture dynamics, yields, water availability and economic returns through a series of feedback mechanisms.

The model explicitly links "cropping area – irrigation – soil moisture – yield – economic returns – available water" through endogenous feedbacks within a unified stock–flow structure, rather than treating these components as independent optimisation problems (*Figure 2*). In this way, the model is designed to trace how governance-relevant decisions propagate through coupled biophysical and economic processes over time. Detailed variable definitions are provided in Appendix B.

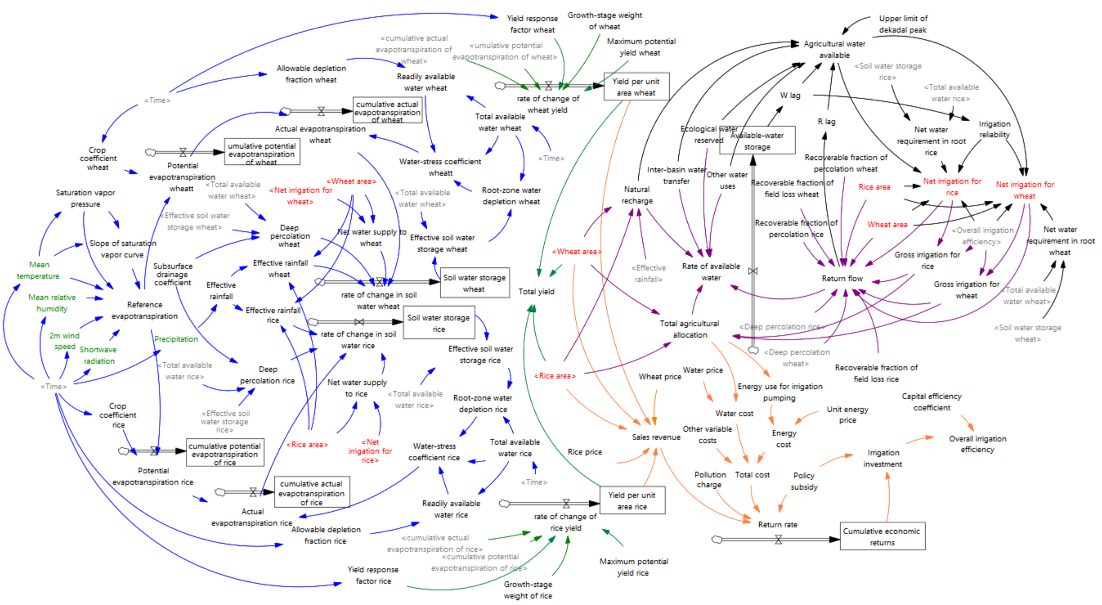

Figure 2 Stock–flow diagram of the system

3.2 Key processes and governing relationships

3.2.1 Soil moisture dynamics and crop water balance

The soil-moisture sub-system represents root-zone water storage for rice and wheat as stock variables at the dekad scale (Basir et al., 2024). Reference evapotranspiration is calculated using the FAO Penman–Monteith formulation, and crop- and stage-specific coefficients are applied to obtain potential evapotranspiration for each crop (Allen et al., 1998; see Appendix A).

Root-zone soil moisture evolves according to a water-balance relationship in which effective precipitation and net irrigation constitute inflow rate variables, while actual evapotranspiration, deep percolation and subsurface drainage constitute outflow rate variables. Water stress is determined by comparing current soil-water depletion with a readily available water threshold. A water-stress coefficient scales potential to actual evapotranspiration, allowing soil-moisture conditions to influence crop water uptake dynamically.

Net irrigation is constrained by both crop water requirements and basin-level water availability. When allocable water is insufficient to satisfy total irrigation demand, an irrigation-reliability coefficient distributes limited supplies across crops in proportion to potential demand. This formulation closes a feedback loop whereby meteorological variability and irrigation decisions jointly determine soil-moisture conditions, which in turn affect subsequent irrigation demand and yield formation.

3.2.2 Crop yield formation

The crop-yield sub-system links soil-moisture dynamics to seasonal yield outcomes using the FAO water–yield response framework. Potential yield is defined under near-optimal water conditions, while actual yield emerges as a state-dependent outcome resulting from the accumulation of evapotranspiration deficits over successive phenological stages.

The growing season is divided into crop-specific growth stages, each characterised by a yield-response factor and weighting coefficient. Stage-level water stress is aggregated to obtain seasonal yield reductions. Model parameters are calibrated so that simulated yields under historical climate and management conditions reproduce observed yield patterns.

Through this structure, yields are not imposed exogenously but emerge endogenously from the interaction between soil-moisture, irrigation decisions and climatic conditions.

3.2.3 Basin-scale available water balance

Available water is represented as a stock variable describing basin-scale allocable water for agriculture use. The magnitude of this stock at each dekad is governed by inflow and outflow rate variables. Inflows include natural recharge, inter-basin transfers and agricultural return flows, while outflows include agricultural withdrawals, ecological releases and other sectoral water uses (Sun et al., 2025).

Natural recharge, inter-basin transfers and non-agricultural demands are treated as exogenous, whereas agricultural withdrawals and return flows are endogenously determined by cropping structure, irrigation depth and irrigation efficiency. Gross withdrawals are derived by adjusting net irrigation for conveyance and application losses, allowing inefficiencies to feed back into basin-scale availability via return flows.

The available water stock functions as an explicit state-dependent constraint on feasible irrigation flows at each dekad. Under wet conditions, irrigation is primarily constrained by crop demand and economics considerations. under drought or persistent over-extraction, declining storage progressively tightens this constraint, forcing trade-offs between crops and growth stages. This mechanism captures how climate trends and policy interventions jointly shape both short-run irrigation choices and medium-run water availability.

3.3 Model calibration and validation

The SD model is calibrated using data from a representative rice–wheat irrigation system in the middle Yangtze region. Calibration parameters include crop coefficients, soil water-holding capacity, irrigation efficiency, potential yields, yield-response factors, cost coefficients and policy parameters.

Crop calendars are derived from regional cultivation guidelines and agrometeorological observations, and potential yields and cost parameters from recent agricultural statistics. Using historical meteorological data and observed crop areas and irrigation practices, the model is run for 2021 and parameters are adjusted within agronomically plausible ranges until simulated yields and total irrigation use fall within acceptable error bounds.

Model validation follows standard system dynamics practice and focuses on behaviour reproduction rather than point prediction. First, a realism test evaluates whether simulated yields and water-use trajectories under observed 2021 meteorological conditions and cropping patterns are consistent with empirical observations. Simulated rice and wheat yields deviate from observed values by approximately ±5% (*Figure 3*), indicating that the model captures key relationships among weather, soil moisture, crop water use and yield outcomes.

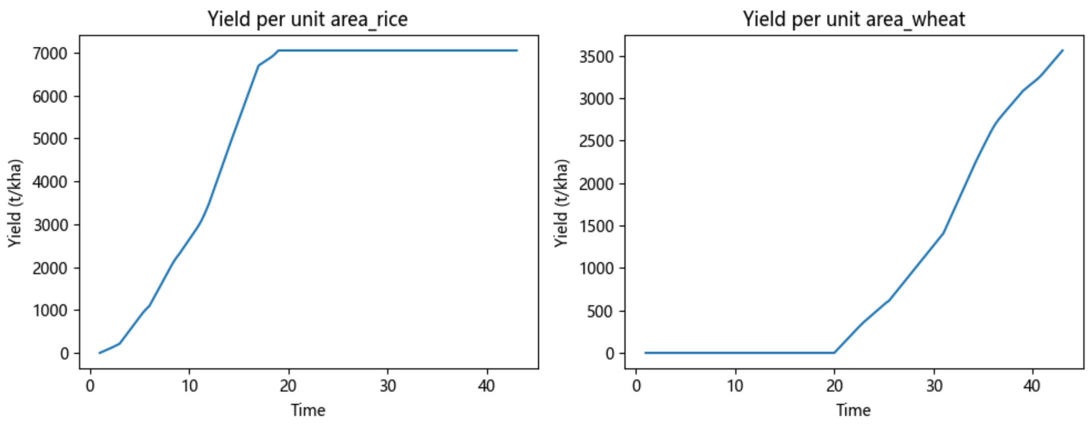

Figure 3 Comparison between simulated and observed yields for 2021

Second, an extreme-condition test examines model behaviour under a stylised extreme-drought scenario with zero precipitation. Under this scenario, available-water storage declines rapidly, irrigation constraints tighten and yields decrease sharply as soil-water deficits accumulate. The model exhibits no negative stocks or unstable dynamics (*Figure 4*), suggesting that its behaviour remains physically and logically consistent under stress conditions.

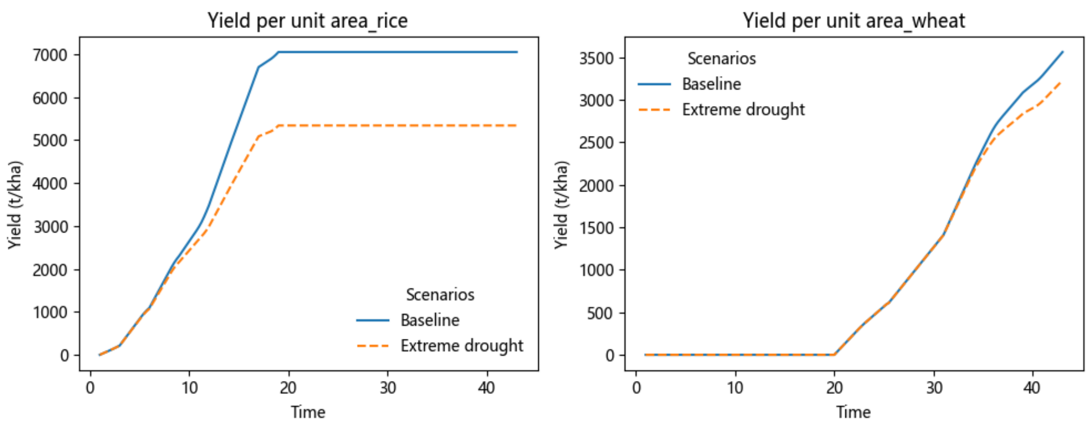

Figure 4 Simulated yield response under the extreme drought scenario

Together, these tests indicate that the SD model provides a robust representation of coupled land–water–economy dynamics suitable for subsequent optimisation and scenario analysis.

4. Multi-objective optimisation

4.1 Objective setting

After calibration and validation, the SD model is embedded within a multi-objective optimization (MOO) framework to identify robust land–water strategies under climate change. Because the coupled land–water system is nonlinear, feedback-rich and characterised by multiple competing objectives, we employ the NSGA-II evolutionary algorithm, which is well suited to approximate non-convex Pareto fronts without gradient information.

The decision vector comprises crop-specific sown areas and dekad-level net irrigation depths for wheat and rice over the planning horizon. For each candidate decision vector, the SD model simulates coupled dynamics of soil water, crop growth, yield formation, economic returns and basin-scale available water under a given climate–policy scenario. Land- and water-balance constraints, upper bounds on total arable land and irrigation water, and minimum area requirements for each crop are imposed as inequality constraints. Infeasible solutions are penalised and gradually eliminated during the evolutionary search.

Three policy-relevant objectives are optimised simultaneously.

First, **total net profit** over the planning horizon captures the primary economic incentive of farmers and local governments.

Second, **irrigation water productivity** (IWP) measures total grain output per unit of gross irrigation, capturing how effectively scarce water is transformed into production.

Third, **yield stability** is represented by cumulative deviation of total production from a baseline level, so that land–water strategies that induce large aggregate production losses are penalised. These objective functions are all presented in Appendix A.

Within NSGA-II, candidate land–water strategies are sampled within the feasible decision space and evaluated by the SD model to obtain profit, IWP and yield-deviation values. Through non-dominated sorting and diversity preservation, the algorithm evolves the population towards the Pareto front that characterises trade-offs among economic returns, water-use efficiency and production stability. This frontier forms the analytical basis for result interpretation in Section 4.2.

4.2 Result analysis

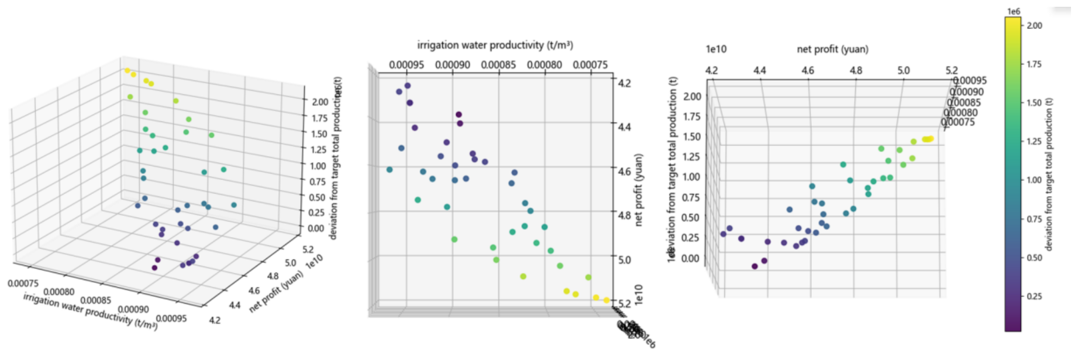

Figure 5 Pareto frontier of the historical baseline model

4.2.1 Trade-offs under the historical baseline

The Pareto frontier under the historical baseline scenario reveals pronounced trade-offs among irrigation water productivity, economic returns and yield stability (*Figure 5*). Configurations that maximise irrigation water productivity tend to achieve lower total profits, while profit-oriented strategies are associated with larger cumulative yield deviations.

Compared with the Baseline Model representing actual 2021 production patterns (*Table 1*), all Pareto-efficient strategies achieve substantial gains in irrigation water productivity—on the order of 14%—demonstrating substantial scope to increase grain output per unit of irrigation water through joint adjustment of cropping area and irrigation allocation under unchanged aggregate land and water constraints. This finding indicates that prevailing land–water configurations are not located near the efficiency frontier, even in the absence of additional technological change.

However, strategies that prioritise profit maximisation do so at the cost of increased pressure on both land and water systems. The profit-oriented solution increases total profit by approximately 5.9% relative to the baseline but simultaneously expands the sown area and induces much larger yield deviations. From a governance perspective, this implies heightened exposure to production risk and resource stress, particularly under climatic variability.

Table 1 Performance comparison with the baseline model

Scheme	IWP (t/m^3)	Profit (billion yuan)	Yield deviation (10^4 t)
Baseline	0.000838	42.67	0
Profit-oriented	0.000953 (+13.6%)	45.21 (+5.9%)	124.3
Knee point / Water-saving-oriented	0.000956 (+14.0%)	42.70 (+0.1%)	76.7

By contrast, the knee-point solution on the Pareto frontier achieves irrigation water productivity gains comparable to those of the most water-efficient configurations while maintaining total profit at baseline levels. Importantly, this solution slightly reduces total sown area and markedly lowers cumulative yield deviation relative to the profit-oriented alternative. As such, it represents a balanced land–water strategy that improves efficiency without exacerbating production instability or resource pressure.

4.2.2 Governance-relevant interpretation of optimisation outcomes

The structure of the Pareto frontier suggests that efficiency gains in irrigation water use are not inherently incompatible with economic viability. Rather, the principal tension arises between short-term profit maximisation and production stability under constrained land and water resources. Profit-oriented strategies implicitly rely on expanded land use and intensified water withdrawals, which may be viable under favourable conditions but amplify vulnerability to drought and water scarcity.

The knee-point configuration illustrates the existence of land–water strategies that reconcile moderate economic performance with enhanced water-use efficiency and reduced yield volatility. From a policy perspective, such strategies align more closely with objectives of sustainable agricultural intensification, where incremental efficiency gains are prioritised over maximal exploitation of land and water.

Importantly, these results highlight that optimisation alone does not prescribe a single "optimal" strategy. Instead, it delineates a feasible space of trade-offs within which policy choices must be made. The Pareto frontier therefore serves as a diagnostic tool for governance, clarifying the opportunity costs associated with privileging profit, efficiency or stability under given institutional and resource constraints.

5. Extended results: framework coupling and future baseline analysis

5.1 Coupling of ML-based climate scenarios, system dynamics and optimisation

This section extends the analysis by examining future baseline conditions using a coupled machine-learning (ML), system dynamics (SD) and multi-objective optimisation framework. The overall analytical structure is illustrated in *Figure 6*, which shows the one-way transfer of climatic forcing from the ML module to the SD model and the iterative feedback between the SD model and the NSGA-II optimisation algorithm.

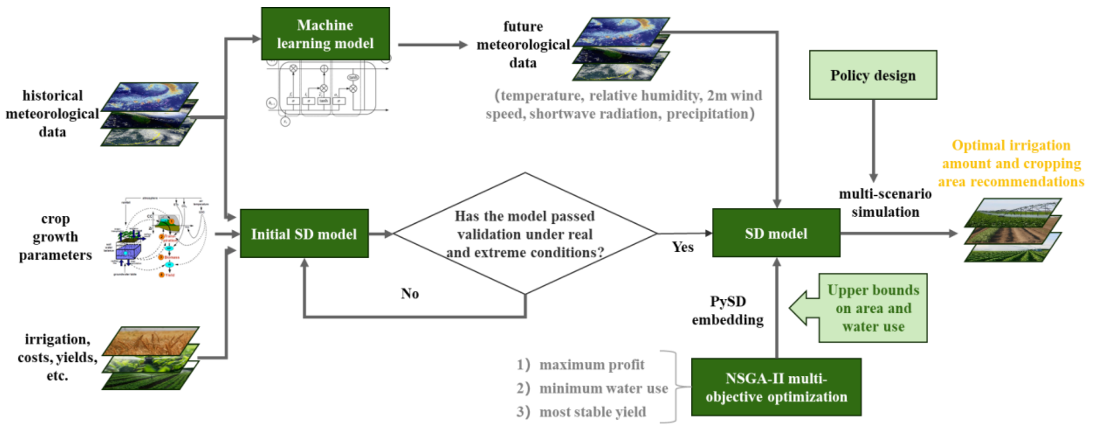

Figure 6 interaction model between models

Within this framework, ML models generate multi-year meteorological sequences that preserve observed seasonality, inter-annual variability and extreme-event characteristics. These climate series are treated as exogenous drivers and introduced into the SD model, where they influence soil moisture dynamics, crop growth, basin-scale available water and economic returns through explicit stock–flow relationships. For each candidate land–water strategy proposed by NSGA-II, the SD model simulates system behaviour over the planning horizon and returns performance metrics to the optimisation algorithm.

The coupling allows systematic exploration of trade-offs among irrigation water productivity, economic returns and yield stability under future climatic conditions. Rather than producing a single optimal solution, the framework identifies a set of Pareto-efficient strategies that characterise the feasible space of land–water decisions under uncertainty.

5.2 Reliability of ML-generated climatic forcing

The credibility of future baseline simulations depends on the adequacy of the ML models used to generate meteorological inputs (Wi and Steinschneider, 2022). The predictive performance of the selected ML models is summarised in *Table 2*, which reports accuracy metrics for key climate variables relevant to crop water demand and evapotranspiration.

As shown in *Table 2*, Ridge regression reproduces the seasonal dynamics of relative humidity and shortwave radiation with low error, while the HistGradientBoostingRegressor captures nonlinear temperature patterns that are critical for reference evapotranspiration estimation. Wind-speed variability is represented using gradient-boosted regression trees with Huber loss, and precipitation dynamics are modelled using a combined GBRT–Tweedie approach that accounts for both extreme events and cumulative rainfall behaviour.

Table 2 Quantitative results of meteorological forecasts

Key variables	Model	MAE	RMSE	sMAPE(%)
Average humidity	Ridge	4.35	5.70	5.61
Total solar irradiance	Ridge	4.26	5.68	33.60
Average temperature	HGBR	1.97	2.55	13.85
2m wind speed	GBRT	1.83	2.42	21.74
Cumulative precipitation (short)	GBRT	3.53	6.23	128.48
Cumulative precipitation (long)	Tweedie	3.73	5.66	127.98

These results indicate that the ML-generated climate series are sufficiently reliable for use as scenario inputs in multi-year land–water simulations. Importantly, the role of the ML module is not to predict specific future weather realisations, but to generate internally consistent climatic trajectories that enable stress testing of land–water strategies under plausible future conditions.

5.3 Future baseline optimisation outcomes

Using the ML-generated climate series as forcing, the coupled SD–optimisation framework is applied to derive Pareto-efficient land–water strategies under future baseline conditions. The resulting solution set reveals systematic trade-offs among irrigation water productivity, economic returns and yield stability.

Across the Pareto-efficient solutions, configurations that prioritise higher water productivity tend to sacrifice economic returns, while profit-oriented strategies are associated with greater production variability. Solutions located near the knee of the Pareto frontier represent balanced strategies that improve irrigation water productivity without incurring disproportionate yield instability. These results provide a reference benchmark for subsequent region-specific and policy-focused analyses.

6. Regional multi-objective optimisation results for Hubei Province

6.1 Baseline model set-up and regional constraints

Daily meteorological series for the period 2025–2029 are first generated using the trained machine-learning models described in Section 5 and then introduced into the system dynamics framework. These time series provide the climatic forcing for all simulations reported in this section.

Regional land and water resource constraints are calibrated using agricultural and water statistics for Hubei Province. Key parameters describing arable land availability, irrigation water supply and historical utilisation levels are summarised in *Table 3*. These values define upper and lower bounds for cropping area and irrigation allocation and are held constant across all scenarios examined in Section 6.

Based on the regional constraints reported in *Table 3* and the ML-generated meteorological inputs, a future baseline model is constructed to represent the land–water system under current management practices and anticipated climate conditions. This baseline provides a reference against which alternative climate and policy scenarios are evaluated in subsequent analyses.

Table 3 Statistical data for Hubei Province, 2018–2023

Year	Total area (kha)	Annual growth rate of area	Agricultural water use (10^8 m^3)	Annual growth rate of water use
2018	3,496.0	–	150.66	–
2019	3,304.5	–5.48%	153.06	+1.59%
2020	3,312.1	+0.23%	136.17	–11.04%
2021	3,324.7	+0.38%	174.45	+28.11%
2022	3,295.3	–0.88%	192.46	+10.32%
2023	3,312.6	+0.53%	186.51	–3.09%

6.2 Multi-objective optimisation results under regional constraints

Subject to the regional land and water constraints defined in *Table 3*, the NSGA-II algorithm is applied to derive Pareto-optimal land–water strategies for Hubei Province over the 2025–2029 planning horizon. The resulting Pareto frontier is presented in *Figure 7*.

As shown in *Figure 7*, the feasible solution space is substantially narrower than that obtained under the future baseline analysis in Section 5, reflecting the binding effects of regional land and water limitations. The frontier reveals clear trade-offs among irrigation water productivity, economic returns and yield stability. Solutions located toward the profit-maximisation end of the frontier are associated with higher water withdrawals and increased production variability, while water-saving solutions achieve higher irrigation water productivity at the expense of economic returns.

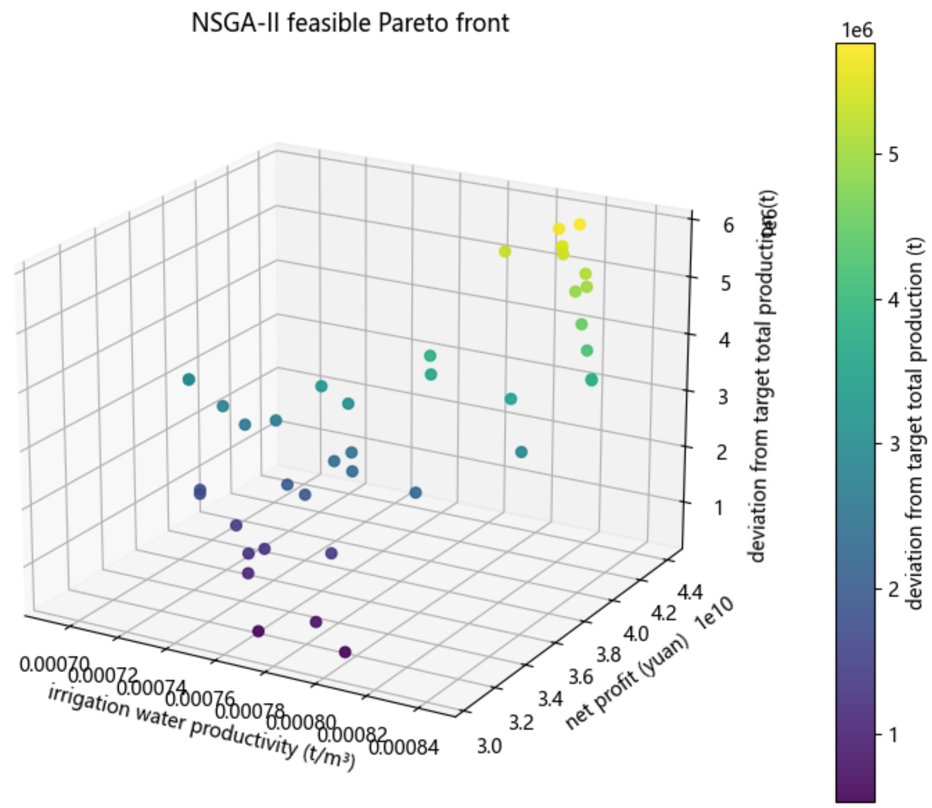

Figure 7 Pareto frontier for the future scenario

More specifically, profit-oriented solutions prioritise economic returns while exhibiting lower irrigation water productivity and greater yield variability. In contrast, water-saving solutions maximise irrigation water productivity but entail notable reductions in total economic returns. A knee-point solution identified on the Pareto frontier in *Figure 7* represents an intermediate configuration that moderates these trade-offs, achieving balanced performance across irrigation water productivity, economic returns and yield stability.

Relative to the more extreme solutions along the frontier, the knee-point configuration reduces irrigation demand and stabilises yields while maintaining acceptable economic performance. This solution is therefore selected as the reference configuration for subsequent climate and policy scenario comparisons in Section 6.3.

6.3 Climate and policy scenario comparison

To assess the robustness of land–water strategies under different climatic and policy conditions, additional scenarios are simulated for Hubei Province, including reduced-precipitation (drought) conditions and alternative policy instruments. Specifically, scenarios incorporating irrigation quotas, block water pricing and combined policy packages are examined.

Key performance indicators for all climate–policy combinations are reported in *Table 4*, including irrigation water productivity, total economic returns and yield stability. Under normal climatic conditions, *Table 4* shows that policy instruments induce moderate improvements in water-use efficiency while maintaining production and income levels close to the future baseline. These effects are achieved primarily through reallocation of irrigation water toward higher-marginal-return uses.

Under drought conditions, the results in *Table 4* indicate substantial declines in both yields and economic returns across all policy scenarios. Although quota-based and pricing policies partially mitigate income losses, they do not prevent significant reductions in irrigation during critical crop growth stages. Differences among policy regimes narrow markedly under drought, highlighting the dominance of biophysical constraints over marginal economic incentives when water availability becomes severely limited.

Table 4 Comparison of key indicators across scenarios

Scenario	IWP (t/m^3)	Net profit (billion yuan)	Total yield deviation (10^4 t)
Future Baseline	0.000831	37.45	0
Policy adjustment	0.000833 (+0.2%)	36.72 (–1.9%)	38.7
Extreme drought	0.000702 (–15.5%)	27.51 (–26.6%)	400.4
Extreme drought + policy adjustment	0.000706 (–15.0%)	27.53 (–26.5%)	393.9

Taken together, the multi-scenario results reported in *Table 4* demonstrate that while policy instruments can influence irrigation behaviour under moderate conditions, their effectiveness is fundamentally constrained under extreme climatic stress in Hubei Province.

7. Conclusions

This study develops an integrated ML–SD–NSGA-II framework to analyse and optimise trade-offs among the coupled challenges of yield stability, water scarcity and income growth in irrigated agriculture under climate change. The framework links ML-based meteorological scenario generation, SD simulation of crop–water–economy interactions and multi-objective optimisation within a unified decision-support system, using a humid monsoon rice–wheat double-cropping region in central China as a representative case with potential transferability to other irrigated basins.

Under current-climate conditions, comparison with the observed baseline reveals substantial untapped efficiency. Representative Pareto-optimal schemes increase irrigation water productivity by about 14% without relaxing land or water constraints. A profit-oriented configuration increases net revenue by about 6% but expands sown area and amplifies yield deviation, implying greater exposure to climate risk and land pressure. By contrast, a knee-point configuration maintains near-baseline profit while improving water-use efficiency, slightly reducing sown area and markedly lowering yield deviation, indicating that coordinated adjustment of cropping structure and irrigation allocation can deliver “more grain per drop” without sacrificing income.

Future scenario analysis clarifies the differentiated role of economic instruments under climate stress. Under differentiated volumetric pricing and otherwise normal weather, water-use efficiency improves modestly, profits decline only slightly and yield deviations remain small, indicating that tariffs calibrated to local conditions can curb low-value irrigation while safeguarding supply during critical growth stages. Under an extreme-drought analogue, sharp reductions in effective water availability lead to simultaneous deterioration in efficiency, profit and yield stability. In this context, the addition of quotas and block tariffs yields only marginal improvements, indicating that prices and subsidies primarily facilitate buffering and reallocation and cannot offset absolute water scarcity. Structural measures, including drought-tolerant varieties, upgraded irrigation technologies and reconfigured crop portfolios, therefore remain indispensable.

Methodologically, the study demonstrates how a transferable ML–SD–NSGA-II framework can shift SD-based analysis from ex post scenario exploration toward ex ante multi-objective decision support, and how treating yield deviation as an explicit objective helps make trade-offs among economic returns, resource efficiency and robustness to climatic extremes transparent for policy deliberation. Practically, the optimised schemes provide concrete land–water configurations that improve water productivity while maintaining acceptable income and yield stability, and the standardised “forecast–simulate–optimise” workflow can be adapted to other climate-sensitive irrigation regions to inform tariff design, subsidy rules and basin allocation.

Nevertheless, several limitations remain. The analysis is calibrated to a single humid monsoon system, adopts a simplified representation of groundwater processes and compound extremes, and relies on ML-based climate scenarios. Future research should extend the framework to semi-arid and groundwater-dependent basins, explicitly couple surface–groundwater regulation and water-rights trading, and incorporate ensemble climate projections to assess the robustness of policy-relevant trade-offs.

References

Ahmed AA, Sayed S, Abdoulhalik A, et al. (2024) Applications of machine learning to water resources management: A review of present status and future opportunities. *Journal of Cleaner Production* 441: 140715.

Allen RG, Pereira LS, Raes D, et al. (1998) Crop evapotranspiration: Guidelines for computing crop water requirements, FAO irrigation and drainage paper 56. *FAO* 56.

Basir MS, Noel S, Buckmaster D, et al. (2024) Enhancing subsurface soil moisture forecasting: A long short-term memory network model using weather data. *Agriculture* 14(3): 333.

Becker R, Schüth C, Merz R et al. (2023) Increased heat stress reduces future yields of three major crops in Pakistan's Punjab region despite intensification of irrigation. *Agricultural Water Management* 281: 108243.

Cao D, Yi X, Chen X et al. (2022) Water requirement of non-staple crops in the Yellow River Delta based on climate change. *Chinese Journal of Soil Science* 53(4): 795–804 (in Chinese).

Cao X, Huang J, Zhou G, et al. (2025) A review of rice–rapeseed cropping system in China: towards sustainable development. *Crop and Environment* 4(3): 192–202.

Demir MS and Muratoglu A (2025) Optimisation of agricultural crop pattern based on water footprint methodology. *Integrated Environmental Assessment and Management* 21(5): 1110–1123.

Deng Y and Zhang L (2025) Water rights trading and agricultural water use efficiency: Evidence from China. *Water* 17(14): 2047.

Dong H, Chen X, Feng S et al. (2022) Effects of climate change on seed yield and water use efficiency of cotton in arid regions: A simulation study. *Journal of Irrigation and Drainage* 41(9): 23–32, 51 (in Chinese).

FAO (2011) The state of the world's land and water resources for food and agriculture (SOLAW): Managing systems at risk. Rome: FAO and Earthscan.

Feng Y, Guo Y, Shen Y, et al. (2024) Change of crop structure intensified water supply-demand imbalance in China's black soil granary. *Agricultural Water Management* 306: 109199.

Feng Z, Du C, Zhang J et al. (2023) Research advances of water-saving irrigation technology and water use efficiency in China and Europe. *Plant Physiology Journal* 59(9): 1735–1748 (in Chinese).

Ghimire P, Karki S, Pandey VP, et al. (2025) Mapping spatio-temporal dynamics of irrigated agriculture in Nepal using MODIS NDVI and statistical data with Google Earth Engine: A step towards improved irrigation planning. *International Journal of Applied Earth Observation and Geoinformation* 136: 104345.

Guemouria A, Chehbouni A, Belaqziz S, et al. (2023) System dynamics approach for water resources management: A case study from the Souss-Massa Basin. *Water* 15(8): 1506.

He L, Du B, Xiong L, et al. (2025) Enhancing food security and farmers' profit through ratoon rice-potato rotation in central China. *European Journal of Agronomy* 168: 127636.

IPCC (2021) Climate change 2021: The physical science basis. Contribution of Working Group I to the Sixth Assessment Report of the Intergovernmental Panel on Climate Change. Geneva: Intergovernmental Panel on Climate Change.

IPCC (2022) Climate change 2022: Impacts, adaptation and vulnerability. Contribution of Working Group II to the Sixth Assessment Report of the Intergovernmental Panel on Climate Change. Cambridge: Cambridge University Press.

Jamali M, Yazdian H, Bahman G, et al. (2025) Water agriculture nexus a system dynamics approach for the next three decades. *Scientific Reports* 15(1): 5946.

Jia Y, Liu Z and Tang L (2023) Using system dynamics to improve agricultural water use efficiency in Qingtongxia Irrigation District. *Journal of Irrigation and Drainage* 42(4): 137–144 (in Chinese).

Lesk C, Anderson W, Rigden A, et al. (2022) Compound heat and moisture extreme impacts on global crop yields under climate change. *Nature Reviews Earth & Environment* 3(12): 872–889.

Li M, Li H, Zhou Z, et al. (2024) Spatial simulation and optimisation of cropping structure under climate and land use change conditions considering synergistic economic benefits and carbon reduction in crop growth processes. *Earth's Future* 12(10): e2024EF004684.

Li Y and Liu J (2020) Prospects for development of water-saving irrigation equipment and technology in China. *Journal of Drainage and Irrigation Machinery Engineering* 38(7): 738–742 (in Chinese).

Liu Q, Niu J, Du T, et al. (2023) A full-scale optimisation of a crop spatial planting structure and its associated effects. *Engineering* 28: 139–152.

Lopes GR, Bastos Lima MG and dos Reis TNP (2021) Maldevelopment revisited: Inclusiveness and social impacts of soy expansion over Brazil's Cerrado in Matopiba. *World Development* 139: 105316.

Madani K (2014) Water management in Iran: what is causing the looming crisis? *Journal of Environmental Studies and Sciences* 4(4): 315–328.

Mall RK, Singh R, Gupta A, et al. (2006) Impact of climate change on Indian agriculture: A review. *Climatic Change* 78(2–4): 445–478.

Marcinkowski P, Piniewski M and Okruszko T (2024) Towards sustainable agricultural water management in Poland - How to meet water demand for supplemental irrigation? *Agricultural Water Management* 306: 109214.

McGuire VL (2014) Water-level changes and change in water in storage in the High Plains Aquifer, predevelopment to 2013 and 2011–13. Reston, VA: U.S. Geological Survey.

Mehrazar A, Massah Bavani AR, Gohari A, et al. (2020) Adaptation of water resources system to water scarcity and climate change in the suburb area of megacities. *Water Resources Management* 34(12): 3855–3877.

Naeem K, Aloui S, Zghibi A, et al. (2024) A system dynamics approach to management of water resources in Qatar.

Sustainable Production and Consumption 46: 733–753.

Nesanır MO, Zenezini G, Senvar O, et al. (2026) A literature review on the integration of system dynamics and machine learning/artificial intelligence in addressing environmental matters. In: *Advances in Production Management Systems. Cyber-Physical-Human Production Systems: Human-AI Collaboration and Beyond* (eds H Mizuyama, E Morinaga, T Nonaka, et al.), Cham, 2026, pp. 370–384. Springer Nature Switzerland.

Ortuzar I, Serrano A, Xabadia A, et al. (2025) Balancing efficiency and inequality in a non-linear multi-regional water allocation optimisation model. *Environmental and Resource Economics* 88(3): 761–794.

Qi P, Sun J and Zhang G (2025) Optimal allocation of water and land resources considering crop water demand process from the perspective of water-carbon-economy nexus. *Journal of Hydrology* 654: 132831.

Reca J, Roldán J, Alcaide M, et al. (2001) Optimisation model for water allocation in deficit irrigation systems I. Description of the model. *Agricultural Water Management* 48(2): 103–116.

Shi R and Guo W (2024) Research progress on the optimal allocation of agricultural irrigation water resources. *Transactions of the Chinese Society of Agricultural Engineering* 40(4): 1–13.

Shi W, Wang M, Tao F, et al. (2024) Wheat redistribution in Huang–Huai–Hai, China, could reduce groundwater depletion and environmental footprints without compromising production. *Communications Earth & Environment* 5(1): 380.

Steward DR, Bruss PJ, Yang X, et al. (2013) Tapping unsustainable groundwater stores for agricultural production in the High Plains Aquifer of Kansas, projections to 2110. *Proceedings of the National Academy of Sciences* 110(37).

Su R, Sui H, Ren G, et al. (2024) Evaluation of crop structure optimisation policy quantitatively and future directions in China: A PMC-index model approach. *Frontiers in Sustainable Food Systems* 8.

Sun L, Dai S, Tian L, et al. (2025) Optimal water allocation considering water diversion projects in an agricultural irrigation district. *Agriculture* 15(9): 949.

Torabi A, Yosefvand F, Shabanlou S et al. (2024) Optimisation of integrated operation of surface and groundwater resources using multi-objective grey wolf optimiser (MOGWO) algorithm. *Water Resources Management* 38: 2079–2099.

Wang W, Li K, Liu Y et al. (2022) A system dynamics model analysis for policy impacts on green agriculture development: A case of the Sichuan Tibetan Area. *Journal of Cleaner Production* 371: 133562.

Wi S and Steinschneider S (2022) Assessing the physical realism of deep learning hydrologic model projections under climate change. *Water Resources Research* 58(9): e2022WR032123.

Wu H, Li Z, Deng X, et al. (2025) Enhancing agricultural sustainability: Optimising crop planting structures and spatial layouts within the water-land-energy-economy-environment-food nexus. *Geography and Sustainability* 6(3): 100258.

Xu L, Xu B, Gao R, et al. (2025) Study on water resource carrying capacity and crop structure optimisation based on gray relational analysis. *Plants* 14(5): 685.

Ye Z, Yin S, Cao Y, et al. (2024) AI-driven optimisation of agricultural water management for enhanced sustainability. *Scientific Reports* 14(1): 25721.

Yin N, Luo S and Xia Y (2025) Policy effects of China's water rights trading on grain production: The role of market incentives in promoting sustainability. *Frontiers in Sustainable Food Systems* 9: 1607156.

Zhao Y, Li G, Li S, et al. (2024) A review on the optimisation of irrigation schedules for farmlands based on a simulation–optimisation model. *Water* 16(17): 2545.

Zhang H (2023) Climate change threatens China's rice bowl. Available at: https://eastasiaforum.org/2023/08/05/climate-change-threatens-chinas-rice-bowl/ (accessed 5 August 2023).

Zhou J, Luo Y, Wang J, et al. (2024) Impacts of planting structure adjustment on water saving in the Shiyang river basin of arid region. *Scientific Reports* 14(1): 30732.

Zou S, Ju H and Zhang J (2025) Water quality management in the age of AI: Applications, challenges, and prospects. *Water* 17(11): 1641.

Appendix A (Calculation formula)

$$L_i(t+\Delta t) = L_i(t) + R_i(t)\Delta t \tag{1}$$

$$1\,mm \cdot ha = 10m^3,\quad Vol(Mm^3) = 0.01 \times Depth(mm) \times A(\text{kha}) \tag{2}$$

$$\boldsymbol{Soil'_{c,t} = P^{eff}_{c,t} + I^{net}_{c,t} - ETs_{c,t} - Perc_{c,t}} \tag{3}$$

$$\boldsymbol{Soil_{c,t+1} = Soil_{c,t} + Soil'_{c,t}} \tag{4}$$

$$\boldsymbol{P^{eff}_{t} = P_t \times \eta^{rain}} \tag{5}$$

$$\boldsymbol{P^{eff}_{c,t} = P^{eff}_{t} \times \frac{A_c}{\sum_c A_c}} \tag{6}$$

$$\boldsymbol{I^{net}_{c,t} = \frac{Irr^{net}_{c,t}}{0.01 \times A_c}} \tag{7}$$

$$\boldsymbol{Depl_{c,t} = TAW_c - Soil^{eff}_{c,t}} \tag{8}$$

$$\boldsymbol{Soil^{eff}_{c,t} = \min\left(TAW_c, \max\left(0, Soil_{c,t}\right)\right)} \tag{9}$$

$$\boldsymbol{RAW_c = TAW_c \times p_c} \tag{10}$$

$$\boldsymbol{Ks_{c,t} = \begin{cases} 1, & Depl_{c,t} \le RAW_c \\ \dfrac{TAW_c - Depl_{c,t}}{TAW_c - RAW_c}, & RAW_c < Depl_{c,t} < TAW_c \\ 0, & Depl_{c,t} \ge TAW_c \end{cases}} \tag{11}$$

$$\boldsymbol{ETs_{c,t} = Ks_{c,t} \times ETc_{c,t}} \tag{12}$$

$$\boldsymbol{ETc_{c,t} = Kc_{c,t} \times ET0_t} \tag{13}$$

$$\boldsymbol{ET0_t = \frac{0.408 \times \triangle \times (Rs_t - G) + \gamma \times \left(\frac{900}{T_t + 273}\right) \times u_{2t} \times RH_t}{\triangle + \gamma \times (1 + 0.34 \times u_{2t})}} \tag{14}$$

$$Perc_{c,t} = \max\left\{0, Soil_{c,t}^{eff} - TAW_c\right\} + \kappa^{drain} \times \max\left\{0, Soil_{c,t}^{eff} - TAW_c\right\} \tag{15}$$

$$\boldsymbol{1 - \frac{Ya_{c,t}}{Ymax_c \times f_{c,t}} = Ky_c \times \left(1 - \frac{\sum_t ETs_{c,t}}{\sum_t ETc_{c,t}}\right)} \tag{16}$$

$$\boldsymbol{Ya_{c,t} = \left[1 - Ky_c \times \left(1 - \frac{\sum_t ETs_{c,t}}{\sum_t ETc_{c,t}}\right)\right] \times Ymax_c \times f_{c,t}} \tag{17}$$

$$\boldsymbol{W_{t+1} = \max\left\{0, W_t + Q_t^{nat} + T_t^{in} + R_t^{ret} - \left(Irr_t^{total} + E_t^{eco} + O_t\right)\right\}} \tag{18}$$

$$\boldsymbol{R_t^{ret} = \sum\nolimits_c [\rho_c^{rf} \times 0.01 \times A_c \times Perc_{c,t} + \rho_c^{ch} \times (Irr_{c,t}^{gross} - Irr_{c,t}^{net})]} \tag{19}$$

$$\boldsymbol{Irr_t^{total} = \sum\nolimits_c Irr_{c,t}^{gross}} \tag{20}$$

$$\boldsymbol{Irr_{c,t}^{gross} = \frac{Irr_{c,t}^{net}}{\eta^{irrig}}} \tag{21}$$

$$\boldsymbol{Irr_{c,t}^{net} = min\left(Req_{c,t}^{net}, \frac{A_c}{\sum_c A_c} \times W_t^{agr}\right) \times \eta^{irrig}} \tag{22}$$

$$\boldsymbol{W_t^{agr} = min\left\{P_{max}, W_{t-1} + Q_t^{nat} + T_t^{in} + R_{t-1}^{ret} - (E_t^{eco} + O_t)\right\}} \tag{23}$$

$$\boldsymbol{\Pi_t = Rev_t - Cost_t + Subsidy_t - Tax_t} \tag{24}$$

$$\boldsymbol{Rev_t = \sum\nolimits_c \mathrm{P}_c^{mk} \times Ya_{c,t} \times A_c} \tag{25}$$

$$\boldsymbol{Cost_t = C_t^{water} + C_t^{energy} + C_t^{var}} \tag{26}$$

$$\boldsymbol{C_t^{water} = \pi^w \times 10^6 \times \sum\nolimits_c Irr_{c,t}^{gross}} \tag{27}$$

$$\boldsymbol{C_t^{energy} = \pi^e \times E_t^{irrig}} \tag{28}$$

$$E_t^{irrig} = \sum\nolimits_c e \times Irr_{c,t}^{gross} \tag{29}$$

$$\max \sum\nolimits_t \Pi_t = \sum\nolimits_t (Rev_t - C_t^{water} - C_t^{energy}) \tag{30}$$

$$IWP = \frac{\sum_t \sum_c Ya_{c,t} \times A_c}{\sum_t \sum_c Irr_{c,t}^{gross}} \tag{31}$$

$$Dev = \sqrt{\sum_{c}(\sum_{t} Ya_{c,t} - Ya_{c}^{*})^{2}} \tag{32}$$

$$Req_{c,t}^{net} = 0.01 \times A_{c} \times I_{c,t}^{net-req} \tag{33}$$

$$I_{c,t}^{net-req} = \max\{0, TAW_{c}, -Soil_{c,t}\} \tag{34}$$

$$0 \leq Irr_{c,t}^{net} \leq Req_{c,t}^{net} \tag{35}$$

$$Irr_{c,t}^{net} \geq \phi_{c,t} \times Req_{c,t}^{net} \tag{36}$$

$$\sum_{t}\sum_{c} Irr_{c,t}^{gross} \leq B_{max} \tag{37}$$

$$\sum_{c} A_{c} \leq A^{total} \tag{38}$$

$$A_{c}, Irr_{c,t}^{net} \geq 0 \tag{39}$$

$$MAE = \frac{1}{n}\sum_{i=1}^{n}|y_{i} - \hat{y}_{i}| \tag{40}$$

$$RMSE = \sqrt{\frac{1}{n}\sum_{i=1}^{n}(y_{i} - \hat{y}_{i})^{2}} \tag{41}$$

$$sMAPE = \frac{100\%}{n}\sum_{i=1}^{n}\frac{|y_{i} - \hat{y}_{i}|}{\frac{|y_{i}| + |\hat{y}_{i}|}{2}} \tag{42}$$

Appendix B

Table 5 Definitions of variables

Variable	Symbol	Unit	Type	Sub-system
Crop	$c \in (rice, wheat)$	-	-	-
Dekad index	$t = 1, \dots, 43$	dekad	-	-
Mean temperature	T_{t}	℃	Exo	Soil moisture
Mean relative humidity	RH_{t}	%	Exo	Soil moisture
2m wind speed	u_{2t}	m/s	Exo	Soil moisture
Shortwave radiation	R_{st}	$MJ/(m^{2} \cdot dekad)$	Exo	Soil moisture
Precipitation	P_{t}	$mm/dekad$	Exo	Soil moisture
Effective rainfall	$P_{c,t}^{eff}$	$mm/dekad$	Aux	Soil moisture
Saturation vapor pressure	e_{s}	kPa	Aux	Soil moisture
Slope of saturation vapor curve	Δ	$kPa/$℃	Aux	Soil moisture
Reference evapotranspiration	$ET0_{t}$	$mm/dekad$	Aux	Soil moisture
Crop coefficient	Kc_{c}	$Dmnl$	Exo	Soil moisture
Potential evapotranspiration	$ETc_{c,t}$	$mm/dekad$	Aux	Soil moisture
Water-stress coefficient	$Ks_{c,t}$	$Dmnl$	Aux	Soil moisture

Variable	Symbol	Unit	Type	Sub-system
Actual evapotranspiration	$ETs_{c,t}$	$mm/dekad$	Aux	Soil moisture
Soil water storage (crop)	$Soil_{c,t}$	mm	Stock	Soil moisture
Effective soil water storage	$Soil_{c,t}^{eff}$	mm	Aux	Soil moisture
Net water supply to crop	$I_{c,t}^{net}$	$mm/dekad$	Aux	Soil moisture
Net irrigation for crop	$Irr_{c,t}^{net}$	$mm/dekad$	Exo	Soil moisture
Deep percolation	$Perc_{c,t}$	$mm/dekad$	Aux	Soil moisture
Total available water	TAW_c	mm	Exo	Soil moisture
Allowable depletion fraction	p_c	$Dmnl$	Exo	Soil moisture
Readily available water	RAW_c	mm	Aux	Soil moisture
Root-zone water depletion	$Depl_{c,t}$	mm	Aux	Soil moisture
Subsurface drainage coefficient	κ^{drain}	$1/dekad$	Exo	Soil moisture
Crop area	A_c	kha	Exo	Soil moisture
Yield per unit area	Ya_c	t/kha	Stock	Crop yield
Maximum potential yield	$Ymax_c$	t/kha	Exo	Crop yield
Yield response factor	Ky_c	$Dmnl$	Exo	Crop yield
Growth-stage weight	$f_{c,t}$	$Dmnl$	Exo	Crop yield
Available-water storage	W_t	Mm^3	Stock	Available water
Agricultural water available	W_t^{agr}	Mm^3	Aux	Available water
Natural recharge	Q_t^{nat}	$Mm^3/dekad$	Aux	Available water
Inter-basin water transfer	T_t^{in}	$Mm^3/dekad$	Exo	Available water
Return flow	R_t^{ret}	$Mm^3/dekad$	Aux	Available water
Ecological water reserved	$E_{c,t}^{eco}$	$Mm^3/dekad$	Exo	Available water
Other water uses	O_t	$Mm^3/dekad$	Exo	Available water
Gross irrigation for crop	$Irr_{c,t}^{gross}$	$Mm^3/dekad$	Aux	Available water
Total agricultural allocation	Irr_t^{total}	$Mm^3/dekad$	Aux	Available water
Overall irrigation efficiency	η^{irrig}	$Dmnl$	Exo	Available water
Recoverable fraction of field loss	ρ_c^{ch}	%	Exo	Available water
Recoverable fraction of percolation	ρ_c^{rf}	%	Exo	Available water
Upper limit of dekad peak	P_{max}	$Mm^3/dekad$	Exo	Available water
Net water requirement in root zone	$I_{c,t}^{net-req}$	$mm/dekad$	Aux	Available water
Cumulative economic returns	Π_t	CNY	Stock	Economic returns
Sales revenue	Rev_t	$CNY/dekad$	Aux	Economic returns
Crop price	P_c^{mk}	CNY/t	Exo	Economic returns
Water price	π^w	CNY/m^3	Aux	Economic returns
Water cost	C_t^{water}	$CNY/dekad$	Aux	Economic returns
Unit energy price	π^e	CNY/kWh	Exo	Economic returns
Energy use for irrigation pumping	E_t^{irrig}	kWh/m^3	Aux	Economic returns
Energy cost	C_t^{energy}	$CNY/dekad$	Aux	Economic returns
Other variable costs	C_t^{var}	$CNY/dekad$	Exo	Economic returns
Total cost	$Cost_t$	$CNY/dekad$	Aux	Economic returns
Pollution charge	Tax_t	$CNY/dekad$	Exo	Economic returns
Policy subsidy	$Subsidy_t$	$CNY/dekad$	Aux	Economic returns